CINSaT Center for Interdisciplinary Nanostructure Science and Technology

Newsletter No. 14 (July 2023)

UNIKASSEL VERSITÄT

Table of Contents

Cover Image

MD Kamrul Hasan (Technological Electronics): A micrograph showing the bubble formation under a metal thin film after oxygen plasma treament with high power.

Preface

Dear reader,

welcome to the first issue of the CINSaT newsletter in 2023. This year started with an important CINSaT member assembly to elect a new executive board, since the term of the previous board ended in 2022. Details about the election and the new board you can find in the General Informations section. As the old and new speaker of the CINSaT I would like to express my gratitude to the CINSaT members for the confidence they have invested in the new executive board. We are motivated to develop the CINSaT forward in the upcoming years.

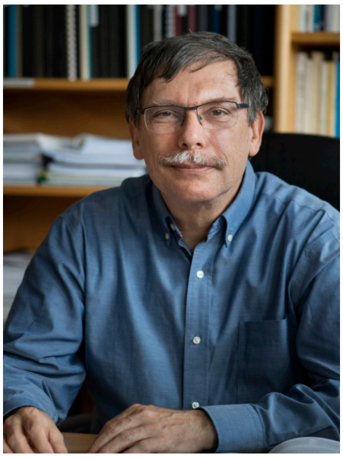

Traditionally, the activities of the CINSaT started with the spring colloquium in Friedrichroda. From 23rd to 24th of February, CINSaT members and their co-workers had the opportunity to meet at the Berghotel Friedrichroda and listening to the scientific program. In over 20 talks and nearly 60 poster contributions the interdisciplinary nature of the CINSaT was showcased once again. During breaks enough room was provided for the participants to discuss different topics and possible collaborations. Read more about the spring colloquium in the Latest Reports section

The main part of the newsletter was of course provided by our members. In the New Projects section, you find information about a new project funded by the ZFF from our member Prof. Raffael Schaffrath (Department of Microbiology). It is utilizing a ‘humanized yeast’ model to investigate the diphthamide modification of elongation factor 2 (EF2) in protein biosynthesis and its ramifications for human health and disease. Dr. Martin Kahlmeyer, part of the group from our member Prof. Stefan Böhm, gives us insight into a planned project about improving the adhesive bonding abilities of titanium surfaces with a pretreatment by laser irradiation inducing nano-structuring of the surface.

In the Research Highlights section Dr. Marilia Horn, part of the group of our member Prof. Thomas Fuhrmann-Lieker, presents a recent publication in collaboration with the group of our member Prof. Hans-Peter Heim, about sustainable plastic alternatives. Polylactic acid (PLA) was blended with unused biomass like chitosan and grape seed, molded into test specimens and their properties were characterized with various methods. This project was supported by the CINSaT in the scope of the Seed Money. Our member Prof. Peter Lehmann presents a publication from his group about the enhancement of the lateral resolution of interference microscopy using annular apertures. This research was realized in collaboration with our member Prof. Thomas Kusserow.

Our member Prof. Cyril Popov recieved an award from the University of Chemical Technology and Metallurgy (UCTM) in Sofia, Bulgaria, for his ongoing efforts to strengthen connections between Germany and Bulgaria in science and education. More informations about the exchange program you can find in the Awards section.

I would like to thank all contributors to this new issue and hope you will enjoy the reading.

General
Latest information from the CINSaT mangement

Here we report briefly about key issues from the CINSaT committees, important discussions, and decisions from their meetings.

Member Meeting

The members met on 28th February 2023. In the following, main issues discussed, and decisions are briefly listed, which are of general interest:

- The financial report was presented by the management and the members released the management with simple majority vote.

- The election term of several members of the executive board ended in 2022. Those members were: CINSaT Speaker Prof. Dr. Johann Peter Reithmaier, Prof. Dr. Thomas Fuhrmann-Lieker, Prof. Dr. Friedrich W. Herberg. Prof. Reithmaier and Prof. Fuhrmann-Lieker declared to stand up for election again. Prof. Herberg decided not be part of the next executive board. Prof. Dr. Arno Müller declared to stand up for election as a representative of the biology. Furthermore, Prof. Dr. Thomas Niendorf decided to stand up for election as well (his term was going until 2024).

- The members voted for the new executive board with simple majority. The board consists of: CINSaT speaker Prof. Reithmaier, Prof. Fuhrmann-Lieker, Prof. Niendorf and Prof. Müller. The election term is 3 years and will end on 28th of February 2026.

- Prof. Dr. Guido Falk von Rudorff and Prof. Dr. Adrian Mellage were accepted as new associated CINSaT members with simple majority vote.

- The associated membership of Prof. Dr. Thomas Kusserow was extended with simple majority vote.

New Members

We welcome two new members to the CINSaT:

- Prof. Dr. Guido Falk von Rudorff has been at the University of Kassel since October 2022 and is developing the "Computational Chemistry of Nanomaterials" department in FB 10. He submitted his application for associated membership on 10th of January 2023, and gave his presentation on 24th of February 2023, as part of the CINSaT Spring Colloquium.

- Prof. Dr. Adrian Mellage has been at the University of Kassel since April 2022 and is building up the "Hydrogeology" department in FB 14. He submitted his application for associated membership on 20th of January 2023, and gave his presentation on 23rd of February 2023 as part of the CINSaT Spring Colloquium.

Both were confirmed by decision of the presidential board on 24th of April 2023, successfully completing the application process.

Research Highlights

Sustainable plastic alternatives - PLA blends with materials from unused biomass

The use of sustainable plastic alternatives is essential in the future society with increasing environmental problems. In order to offer a variety of alternatives and to be able to realize appropriate property profiles, available bioplastics are often blended to develop new materials. Especially for the strongly hydrophobic and brittle material polylactic acid (PLA), the adaptation of the properties is mandatory.

Therefore, the investigations aimed to produce a completely biobased blend based on PLA. On the one hand, the properties were to be improved compared to pure PLA, maintaining its biodegradable character. For this reason, the natural polymer chitosan, obtained by the deacetylation of chitin in the presence of strong alkali, was added to PLA [1]. Chitosan is considered a promising renewable and green polymer, as it is derived from waste sources in the fish industry [2]. In addition, an agro-industrial residue was added to the blend to improve the antioxidant properties of the blends without deteriorating the mechanical and thermal properties. The chosen one was the grape seed extract, mainly composed of proanthocyanidins and potentially other compounds like flavonoids and tocopherol.

For the tests, pre-dried PLA was blended with 5% and 15% chitosan using a twin-screw extruder. In addition, blends containing 1% grape seed extract with and without chitosan were produced. The blends were further processed into test specimens (mini shoulder bars) in an injection moulding process and then subjected to various characterization methods (Figure 1).

First, the antioxidant activity of the grape seed extract, which can be extracted from waste products of juice and wine production, was determined. Using the DPPH method, a percentage inhibition of 78.12 ± 5.03 % and thus an antioxidant effect of the additive was determined.

Thermal characterization was applied to analyze the effect of adding chitosan and grape seed extract on PLA crystallinity degree. Moreover, the glass transition temperature (Tg) is a practical criterion for analyzing the miscibility of the components. As a result of the DSC measurement, phase separation of PLA and chitosan was observed at a chitosan content of 15%. Furthermore, chitosan acts as a nucleating agent, increasing the crystallinity of the PLA. In contrast, the samples with grape seed extract show a lower crystallinity because the mobility of the chains is restricted.

The addition of chitosan also leads to a reduction in thermal stability. While the thermal decomposition of pure PLA still starts at 318.7 °C, the onset temperature is reduced by 10 °C (5 % chitosan) or 25 °C (15 % chitosan) by chitosan. The small amount of grape seed extract does not significantly change thermal stability (Figure 2).

In addition to the thermal properties, the mechanical properties of the blends were investigated (Figure 3). The tensile test carried out makes it clear that the addition of chitosan and grape seed extract leads to a reduction in tensile strength, but this is not statistically significant. Looking at the elongation at break, a significant influence of the chitosan was observed, which led to an apparent reduction in tensile strength. The chitosan content had no significant effect. Similarly, no significant impact of either additive on the modulus of elasticity could be observed, although there was a tendency for a slight increase with increasing chitosan content. This observation is consistent with the slight increase in crystallinity with increasing chitosan content. Adding chitosan thus leads to an embrittlement of the material, which could be due to a low compatibility of both phases.

Figure 1: Injection moulded PLA test specimens with chitosan and grape seed extract

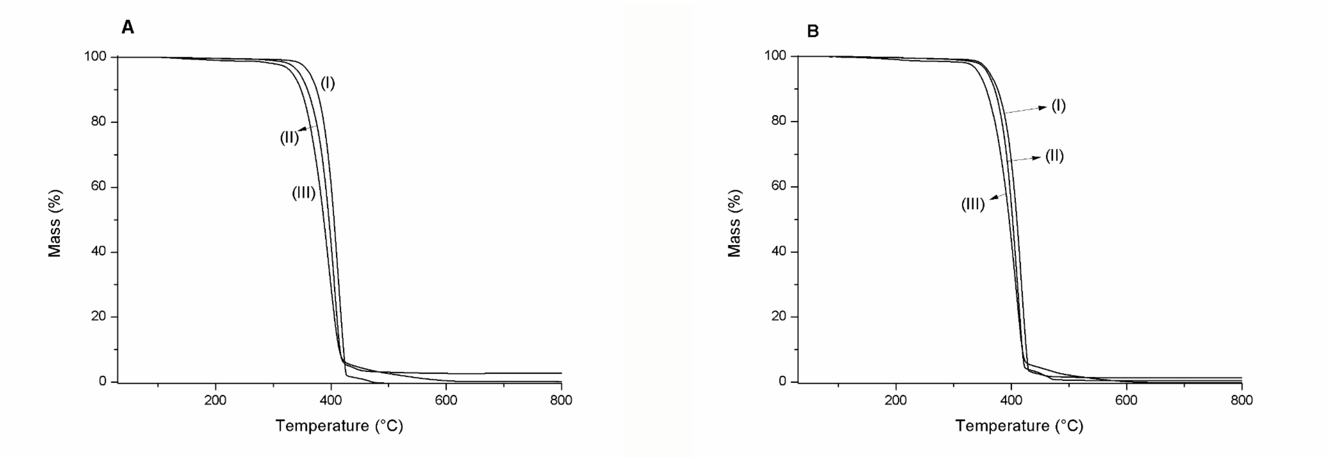

Figure 2: Thermogravimetric curves. In A, samples of PLA and blends with chitosan. In B, samples with grape seed extract [3]

Since including chitosan and red grape seed extract led to an evident change in the colour of the blends, additional colour measurements were carried out. Chitosan leads to an apparent red-yellowish discolouration of the samples, accompanied by a reduction of the L* value (brightness) and a substantial increase of the b* value (yellow). In contrast, all samples containing grape extract show a distinct red-brown colouration, i.e., a reduced L* value (brightness) and an increased a* value (red), regardless of the chitosan content.

In addition, scanning electron microscopy was used to evaluate the surface of the samples. The mixture with chitosan and the addition of the grape seed extract caused the surface to become inhomogeneous, and irregularities and pits were increasingly observed. This observation can be attributed to poor interfacial adhesion.

The investigated materials offer promising end-of-life options for sustainable PLA blends. Grape seed extract showed no significant effect on the thermal and mechanical properties of the blends but improved the antioxidant properties. Conversely, chitosan led to a significant reduction in elongation at break and thermal decomposition.

The work provides initial insights into alternative sustainable blending partners and functional fillers of PLA and thus lays the groundwork for further work in the field of property optimization of bioplastics with biological additives.

Further information

Victoria Goetjes, Claudia L. von Boyneburgk, Hans-Peter Heim and Marilia M. Horn, Polymers 2023, 15, 1570. https://doi.org/10.3390/polym15061570

Acknowledgements

This collaborative project between research groups from FB10 and FB15 was supported by the CINSaT Seed Money Project.

References

[1] Hahn, T.; Tafi, E.; Paul, A.; Salvia, R.; Falabella, P.; Zibek, S. Current state of chitin purification and chitosan production from insects. J. Chem. Technol. Biotechnol. 2020, 95, 2775–2795. [CrossRef]

[2] Águila-Almanza, E.; Low, S.S.; Hernández-Cocoletzi, H.; Atonal-Sandoval, A.; Rubio-Rosas, E.; Violante-González, J.; Show, P.L. Facile and green approach in managing sand crab carapace biowaste for obtention of high deacetylation percentage chitosan. J. Environ. Chem. Eng. 2021, 9, 105229.

[3] Goetjes, V.; von Boyneburgk, C.L.; Heim, H.-P.; Horn, M.M. Influence of Chitosan and Grape Seed Extract on Thermal and Mechanical Properties of PLA Blends. *Polymers* 2023, *15*, 1570. https://doi.org/10.3390/polym15061570

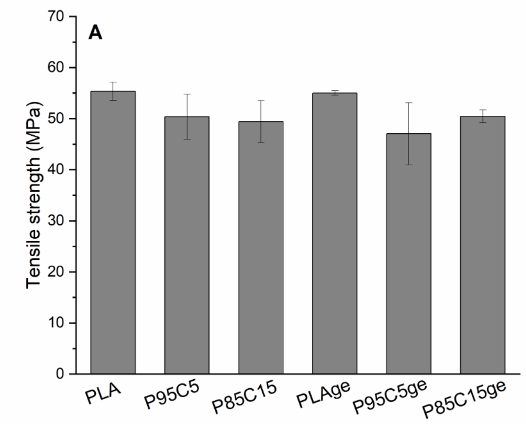

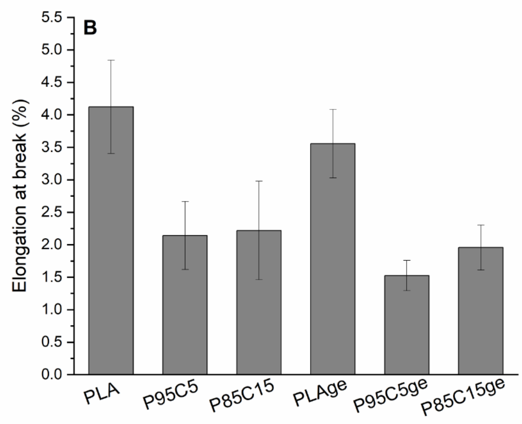

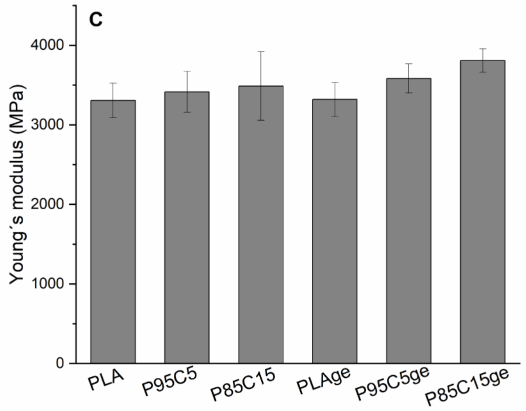

Figure 3: Mechanical properties of PLA and blends measured by tensile tests. In (A), tensile strength; in (B), elongation at break; in (C), Young´s modulus results [3]

Prof. Dr. Hans-Peter Heim
phone: +49 561 804 - 3670
e-mail: heim@uni-kassel.de

Claudia L. von Boyneburgk, M.Sc.
phone: +49 561 804 - 3711
e-mail: c.vonboyneburgk@uni-kassel.de

Victoria Goetjes, M.Sc.
phone: +49 561 804 - 3669
e-mail: victoria.goetjes@uni-kassel.de

Dr. Marilia M. Horn
phone: +49 561 804 - 4101
e-mail: mhorn@uni-kassel.de

Lateral resolution enhancement in interference microscopy by use of virtual annular apertures

The lateral resolution in microscopic imaging is fundamentally limited by the diffraction limit found by Ernst Abbe considering the image formation in a microscope using an optical grating. In contrast, the Rayleigh criterion holds for two individual point sources or point scatterers separated by a certain lateral distance. A portion of each secondary wave occurring at an irregularity is collected by the objective lens and results in an Airy disc corresponding to a diffraction limited intensity point spread function (PSF). If incoherent illumination is employed, the intensity PSFs related to different scatterers on an object are added and their separation is given in terms of the well-known Rayleigh resolution criterion. In interference microscopy instead of the intensity the electric field scattered or diffracted by an object will be affected by the transfer function of the optical imaging system. For a reflective object the lateral resolution of an interference microscope can be again characterized by the Abbe limit if the object under investigation is a grating. However, if two irregularities on a surface are being imaged the resolution no longer obeys the Rayleigh criterion. Instead, it corresponds to an optical system with an annular aperture affecting the electric field and thus surpasses the prediction given by the Rayleigh criterion for a conventional microscope. This holds true for both, amplitude as well as phase objects, as we elucidate by theoretical considerations, simulation results and an experimental proof of principle.

The experimental setup of the used Linnik interference microscope, which is optimized for high lateral resolution, is shown schematically in figure 1 (a). An interference signal called correlogram is obtained during the so-called depth-scan along the z-axis from a plane surface of polished silicon. Figure 1 (b) displays a typical correlogram employing a royal blue LED of 447 nm central wavelength and 20 nm wavelength bandwidth (FWHM) for illumination. The low number of visible interference fringes is due to the high NA of 0.9 of the objective lenses. The absolute value of the Fourier transformed correlogram plotted over the wavelength scale in figure 1 (c) demonstrates that the spectrum of the correlogram is much broader than the spectrum of the light source and extends to wavelengths up to more than 1000 nm.

Changing the distance between the microscope and the object while recording of a series of images results in a 3D image stack, which enables the numerical reconstruction of the surface topography. The transfer characteristics of a depth scanning microscope can be considered by an optical 3D transfer function as it is exemplarily shown in figure 2. The two lateral spatial frequency coordinates of the 3D transfer function (TF) are related to the transversal spatial frequency axes of the microscopic image. The axial spatial frequency distribution results from the interference signals occurring due to the depth scan. Therefore, the lateral spatial frequency distribution of an interference image stack is given by the 3D spatial frequency representation of the complex reflection function of the measuring object weighted by the TF of the interference microscope. In particular, the axial spatial frequency corresponds to the frequency, for which an interference signal of a single camera pixel is analyzed and can thus be varied by appropriate setting of a parameter of the signal processing algorithm, which we call ‘evaluation wavelength’.

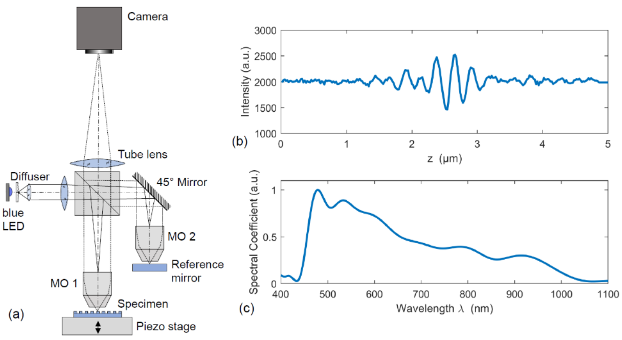

Figure 1: a) Schematic setup of the Linnik interference microscope with royal blue LED light source and two 100x microscope objectives lenses (MO 1 and MO 2) with an NA of 0.9 used throughout this study, b) correlogram obtained from a single camera pixel during the depth scan employing a piezo stage, c) absolute value of the Fourier transform of the correlogram shown in (b) on the wavelength scale.

Since interference signals are typically analyzed at a certain evaluation wavelength corresponding to a certain fringe frequency $q_z = 4\pi/\lambda$, the radius of the outer circular boundary of the transfer function represents the spatial frequency bandwidth of the interference microscope. Obviously, the lateral spatial frequency bandwidth, i.e. the radial extension of a horizontal cross-section through the TF, increases as the evaluation wavelength λ increases. Simulations as well as experimental measurements were performed to confirm the improvement of the lateral resolution capabilities by choosing a high evaluation wavelength.

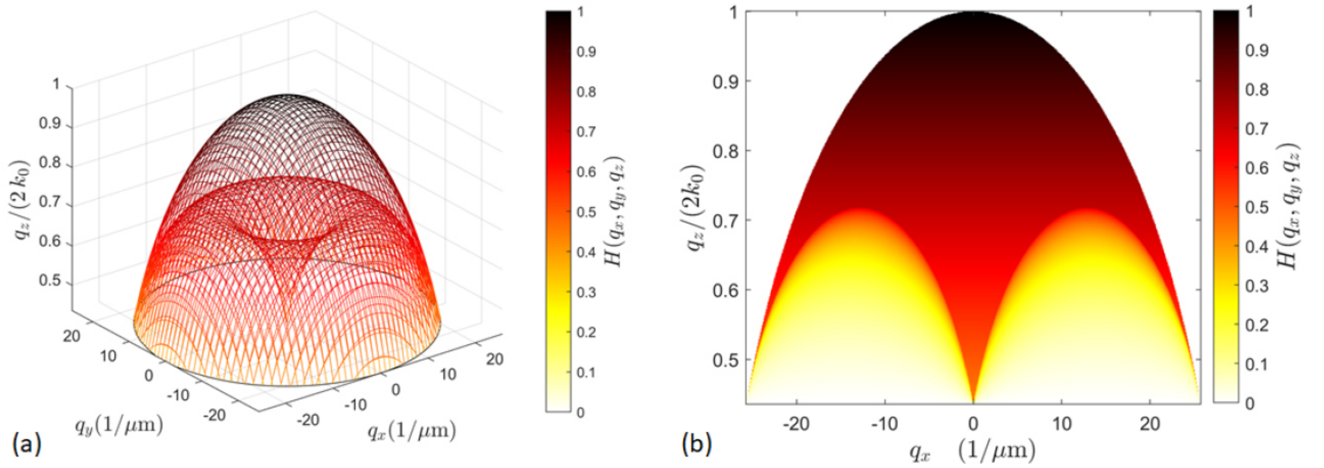

Figure 2: a) Three-dimensional transfer function for monochromatic light of wavelength 447 nm and NA = 0.9. The meshes indicate the upper and lower boundaries of the Ewald limiting sphere. b) cross-sectional view of the transfer function.

It turns out that for grating structures the Abbe limit represents a fundamental limitation even in interference microscopy. On the other hand, if two points on an object are to be resolved, interference microscopy provides a significantly superior lateral resolution compared to conventional microscopy. This is due to the 3D transfer characteristics of an interference microscope, which in contrast to brightfield microscopy gives us access to the axial spatial frequency value via the evaluation wavelength, at which an interference signal is analyzed. In the ideal case the lateral resolution of an interference microscope is approximately 36 % better than the lateral resolution defined according to the Rayleigh criterion in conventional microscopic imaging with spatially incoherent illumination. This is a consequence of the fact that long evaluation wavelengths are due to oblique angles of incidence. Thus, choosing a long evaluation wavelength in the signal analysis algorithm affects the lateral resolution in a similar manner as an annular aperture.

An experimental result is shown in figure 4. The underlying sample was fabricated at INA using a focused ion beam (FIB) system. The individual structures consist of two craters 200 nm apart with a bar of less than 50 nm width in between. Figure 3 is a scanning electron microscope (SEM) image of a cluster of five double craters. Figure 4 (a) and (b) represent results of interferometric phase analysis using an evaluation wavelength of 560 nm (a) and 790 nm (b), respectively. Height profiles corresponding to single columns of figure 4 (a) and (b) are shown in subfigures (c) and (d). The profiles are separated by constant height offsets of 20 nm for better visibility. The double crater structure is not resolved if conventional signal analysis using an evaluation wavelength of 560 nm is employed. However, it can be clearly recognized if the signals are analyzed at an evaluation wavelength of 790 nm. This confirms the fact, that different maximum spatial frequency bandwidths appear, which according to the transfer function depend on the evaluation wavelength introduced before.

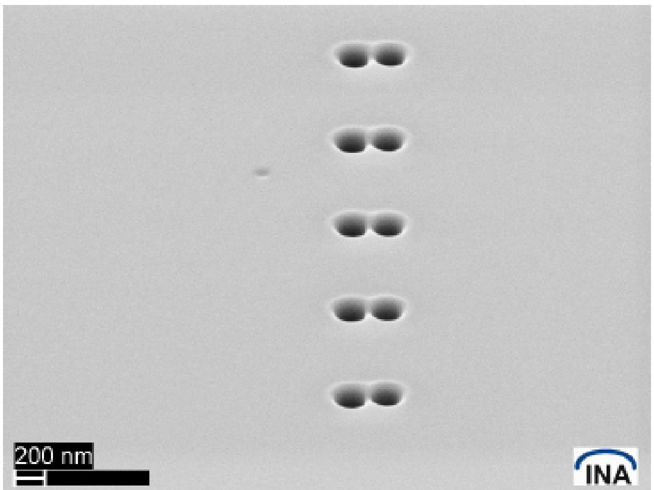

Figure 3: SEM image of a silicon sample with double crater structures of distance d = 200 nm.

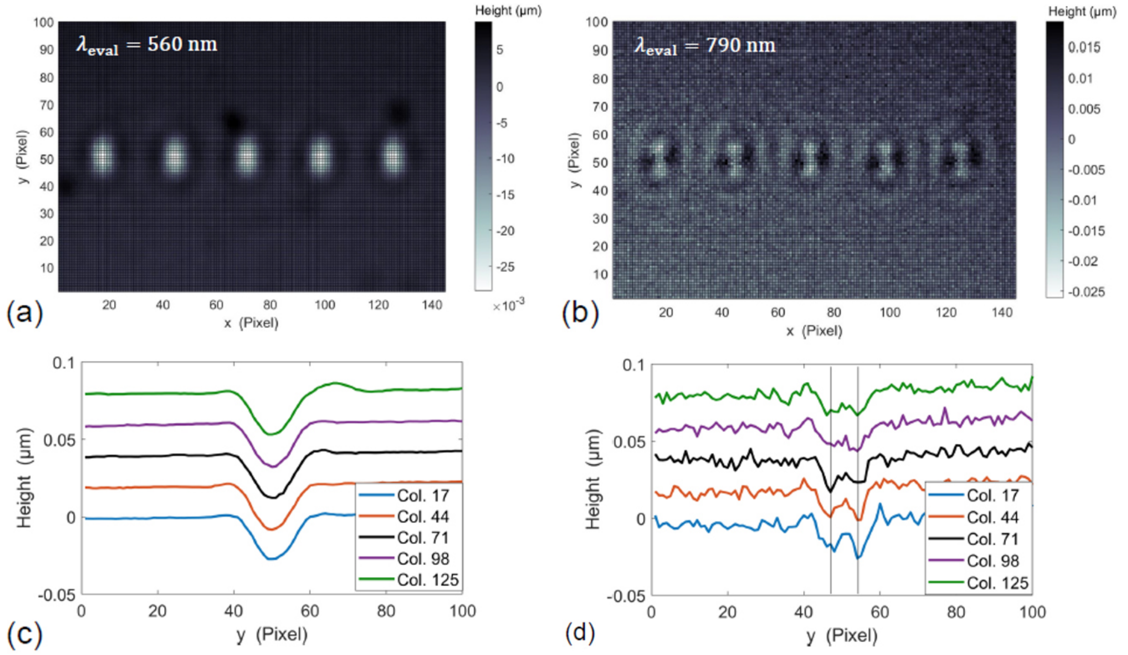

Figure 4: Experimental results for the silicon sample shown in Figure 3: (a) and (b) detailed views representing results of interferometric phase analysis for an evaluation wavelength of 560 nm and 790 nm, (c) and (d) height profiles along the columns according to the legend, separated by constant height offsets of 20 nm for better visibility, corresponding to 560 nm evaluation wavelength (c) and 790 nm evaluation wavelength (d); the locations of the craters are indicated by vertical lines.

Further information

Peter Lehmann, Lucie Hüser, Andre Stelter, Thomas Kusserow, Lateral resolution enhanced interference microscopy using virtual annular apertures, *JPhys Photonics* 5(1) 015001, 2023

Prof. Dr. Thomas Kusserow
phone: +49 561 804 - 4315
e-mail: kusserow@ina.uni-kassel.de

Prof. Dr. -Ing. habil. Peter Lehmann
phone: +49 561 804 - 6313
e-mail: p.lehmann@uni-kassel.de

Andre Stelter, M.Sc.
phone: +49 561 804 - 6413
e-mail: andre.stelter@uni-kassel.de

Lucie Hüser, M.Sc.
phone: +49 561 804 - 6505
e-mail: lucie.hueser@uni-kassel.de

New Projects

Diphthamide, a decider of life & death for translation factor EF2?

The Division of Microbiology led by Professor Schaffrath uses *Saccharomyces cerevisiae*, a yeast model for eukaryotic cell biology, to study modifications on biomolecules that influence mRNA translation, protein synthesis and cell growth.

In all domains of life, radical S-adenosyl-methionine (RS) enzymes use iron-sulfur (FeS) clusters and often modify biological macromolecules (i.e., lipids, proteins, nucleic acids). One such unique protein modification known as diphthamide is conserved from yeast to human cells [1]. It decorates elongation factor 2 (EF2), which helps decode genetic information to make new proteins by ribosomes (aka mRNA translation). Thus, EF2 is essential for all living cells and organisms including our own.

Diphthamide has been linked to diphtheria (hence the name for the EF2 décor), the human infectious disease caused by bacterial diphtheria toxin (DT) [2]. Here, DT hijacks diphthamide to inactivate EF2, block mRNA translation and kill the intoxicated cell (Fig. 1) [2]. The deadly attack by DT represents a complex biochemical reaction. It involves the ADP ribosyl transferase (ART) activity of DT for irreversible modification (i.e., ADP ribosylation) of EF2 (Fig. 1). The reaction requires cofactor NAD^+ as ADP ribosyl donor and diphthamide as acceptor on EF2. Although the DT attack demonstrates a pathological role for diphthamide, its biological function for the cell is less clear. However, drastic consequences that result from diphthamide defects in humans and a gene network (*DPH1-DPH7*) dedicated to diphthamide synthesis and conserved throughout evolution (Fig. 2), suggest the décor ought to be physiologically important for the cell, too. Moreover, previous data have shown endogenous ADP ribosylation of EF2 [3] implying a potential cellular ART activity that may depend on diphthamide in analogy to the lethal one displayed by DT.

Therefore, one blue-sky milestone in this ZFF pilot is to identify a cellular ART from a yeast screen. Complementary to ART screening is our second exploration, which aims to genetically mine the interaction landscape of the *DPH1-DPH7* gene network and uncover functional links between diphthamide, EF2 and mRNA translation. Together, the strategy may clarify whether and how diphthamide on EF2 contributes to the making of new proteins, a process that is fundamental to all life on Earth.

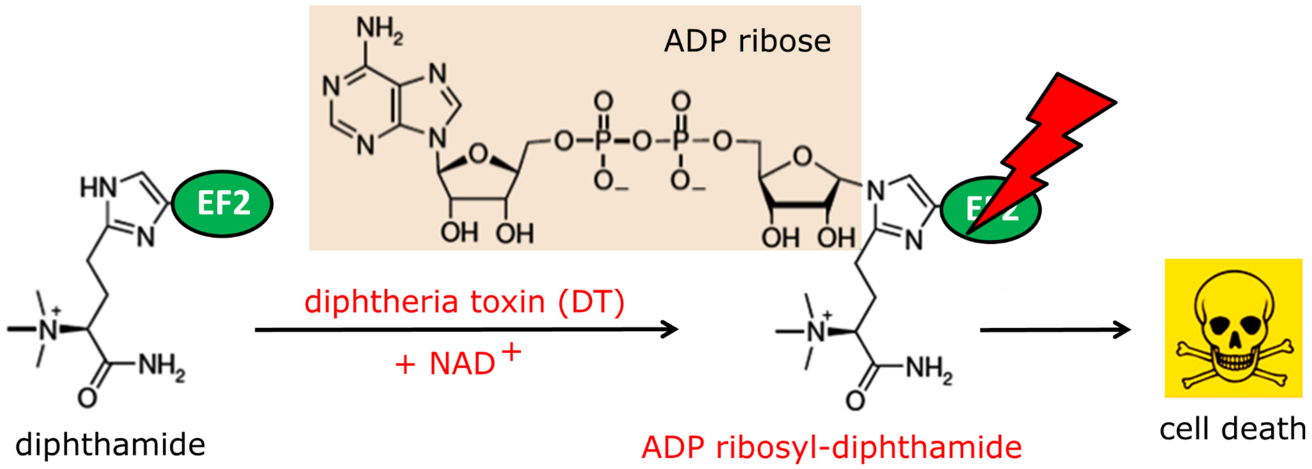

Figure 1: Diphthamide pathology. Diphthamide on EF2 (left) is the site for nicotinamide adenine dinucleotide (NAD^+)-dependent ADP ribosylation by diphtheria toxin (DT). As a result, ADP ribosyl-diphthamide inactivates the essential translation function of EF2 (red bolt), and eventually, causes cell death in diphtheria disease.

The ZFF pilot research idea focusses on diphthamide, an EF2 modification well known for its pathological function in diphtheria. Still its biological role is less clear, and we hardly understand why cells need EF2 to carry diphthamide. Nonetheless, over the last 15 years, independent research teams including our own at the Universities of Halle, Leicester (UK) and Kassel, have dissected a pathway for diphthamide synthesis that is conserved from yeast to human cells (Fig. 2). It involves four steps and a network of genes (*DPH1-DPH7*) [1], whose products modify EF2 with diphthamide at the critical and conserved histidine residue (Fig. 2). Conservation together with findings that human diseases can associate with failure to make proper diphthamide strongly suggest diphthamide is physiologically relevant [4,5]. In further support of such relevance are independent findings from Prof Leppla (NIH, USA) and our own group showing that diphthamide synthesis gene *DPH3* communicates with the Elongator pathway (Fig. 3). The latter is another RS enzyme complex that modifies transfer RNAs (tRNAs), which are molecules indispensable to life for they read the genetic code on mRNAs during the making of new proteins [1,5]. Thus, there is good reason for us to anticipate that tRNA and EF2 modifications may cooperate (Fig. 3) and support healthy cell proliferation and development, particularly in higher organisms.

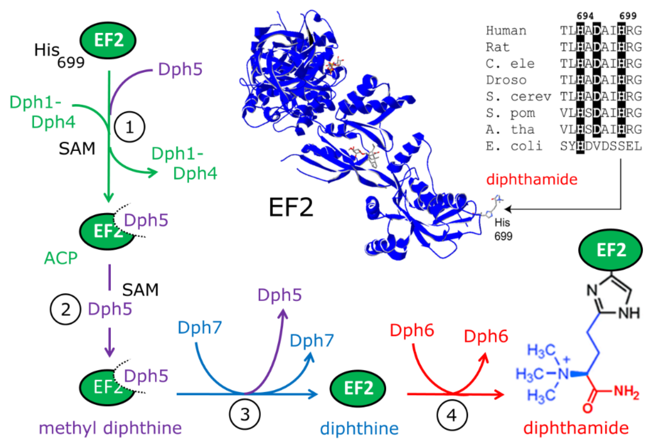

Figure 2: Diphthamide biosynthetic pathway. Diphthamide synthesis involves a four-step pathway conserved in eukaryotes (top right: yeast EF2 structure and diphthamide target site [His-699] aligned to other organisms). It starts (1) with transfer of a 3-amino-3-carboxypropyl (ACP) group from SAM to the imidazole ring of His-699 in EF2. This involves Dph1-Dph4 forming intermediate ACP. ACP undergoes (2) tetra-methylation by Dph5 to generate methyl-diphthine. Next (3), demethylation via Dph7 yields diphthine, which eventually (4) is converted by amidase Dph6 to the end-product, diphthamide.

With diphthamide and EF2 being involved in cell growth and tumor formation, our project has ramifications for human health and disease. Moreover, the pilot presents an excellent illustration of how genetic blue-sky approaches (e.g., synthetic arrays, suppression screen) can innovate a medically relevant field. Our strategy may lead to gene discovery (i.e., ART) involved in protein modifications (e.g., ADP ribosylation) critical for cell proliferation. As for diphthamide deficiency syndrome [1,5], our project promises to use 'humanized yeast' and diagnose variations of a rare disease.

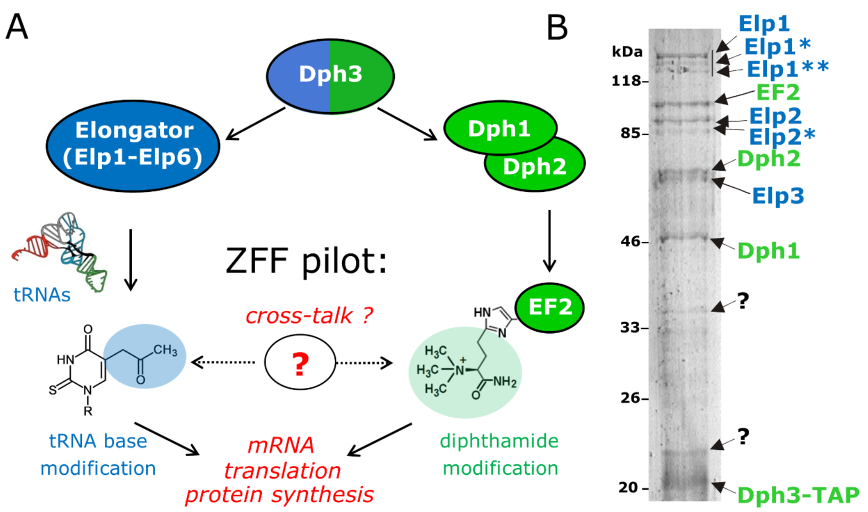

Figure 3: Diphthamide player Dph3 also partakes in tRNA modification. (A) Dph3 drives diphthamide synthesis on EF2 by enzyme Dph1•Dph2 and tRNA base modification by Elongator (Elp1-Elp6). Putative cross-talk (?) between the two pathways and engagement of diphthamide in mRNA translation (?) are central to the ZFF pilot. (B) Tandem affinity purified (TAP) Dph3 interacts with EF2, Dph1•Dph2 and Elongator (Elp1-Elp3). Indicated are unidentified Dph3 partners (?) and Elp1/Elp2 degradation (,**).*

Further information

ZFF – University of Kassel

https://www.uni-kassel.de/uni/forschung/forschungsservice/universitaetsinterne-foerderprogramme/der-zentrale-forschungsfonds-der-universitaet

Professor Schaffrath – home pages

https://www.researchgate.net/profile/Raffael_Schaffrath

https://www.uni-kassel.de/fb10/de/institute/biologie/fachgebiete/mikrobiologie

References

[1] Schaffrath R, Abdel-Fattah W, Klassen R, Stark MJR (2014) The diphthamide modification pathway from Saccharomyces cerevisiae – Revisited. Mol Microbiol 94: 1213-1226.

[2] Collier RJ (1975) Diphtheria toxin: mode of action and structure. Bacteriol Rev 39: 54-85.

[3] Lee H, Iglewski WJ (1984) Cellular ADP-ribosyltransferase with the same mechanism of action as diphtheria toxin and Pseudomonas toxin A. Proc Natl Acad Sci USA 81: 2703-2707.

[4] Hawer H, Mendelsohn BA, Mayer K, Kung A, Malhotra A, Tuupanen S, Schleit J, Brinkmann U, Schaffrath R (2020) Diphthamide deficiency syndrome: a novel human developmental disorder and ribosomopathy. Eur J Hum Genet 28: 1497-1508.

[5] Hawer H, Hammermeister A, Ravichandran KE, Glatt S, Schaffrath R, Klassen R (2019) Roles of Elongator dependent tRNA modification pathways in neurodegeneration and cancer. Genes 10: 19.

Koray Ütkür, M.Sc.
phone: +49 561 804 - 4180
e-mail: k.uetkuer@uni-kassel.de

Prof. Dr. Raffael Schaffrath
phone: +49 561 804 - 4175
e-mail: schaffrath@uni-kassel.de

Improving the bonding ability of titanium surfaces by laser nano-structuring

After processing on air titanium and its alloys form a protective, dense, initially amorphous oxide layer which possess a strong connection to the base material. However, in a warm and humid environment, an oxide may transform into a crystalline modification. This process is associated with a volumetric change of the surface. Thus, if titanium materials are adhesively bonded, this oxide transformation can cause a loss of adhesion and justifies the importance of suitable treatment methods prior adhesive bonding for achieving durable joints.

One approach to overcome the obstacles mentioned is to enhance the adhesion by creating especially porous oxide layers and thus achieving mechanical interlocking of the adhesive at a micro- and nanoscale. With sufficient adhesive infiltration, aging-resistant bonds can be produced, which even withstand the stresses in the interphase caused by the previously described oxide conversion. In addition to wet-chemical methods, pulsed laser systems have proven successful for the creation of such oxide structures in a process incorporating ablation, oxidation in the steam plume and redeposition on the formerly exposed surface. Figure 1 shows an example of a micro- and nanostructured titanium surface created by such a process, using an infrared laser.

Preliminary tests evaluating the strength of the adhesive bond over time have shown that the nanostructures in particular improve the ageing resistance. However, when fracture patterns are observed at high magnification, a partially failure of the oxide layer becomes visible whereas in other areas the nanostructure remains intact (Figure 2).

The framework of a proposed research project aims to clarify which surface structures and adhesive properties are useful for resilient and aging-stable titanium bonds, also under fatigue aspects. First of all, a conflict of objectives must be resolved, i.e. the structure must be well infiltrated by the liquid adhesive, but at the same time should withstand high stresses without delamination. Therefore, it is necessary to examine the relationships between the laser parameters (e.g. pulse duration, fluence, pulse repetition frequency, and focus type) and the generated micro- and nanostructures. The influence of different wetting and infiltration behavior is tested with model adhesives possessing varying viscosities and chemical compositions. The infiltration behavior is evaluated using high-resolution electron microscopy on surfaces exposed by means of an ion beam. In addition, the effect of hygrothermal stress on the interphase, e.g. the oxide transformation – will be investigated.

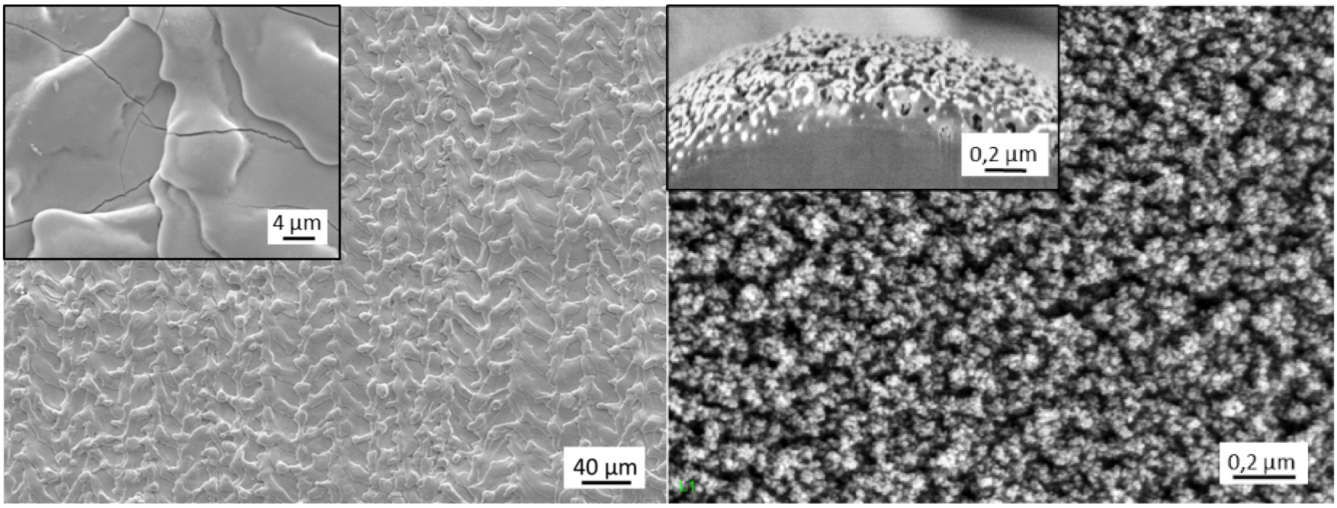

Figure 1: Surface structure on a micro- (left) and nanoscale (right) after laser pretreatment.

With this in mind, adhesive tests are carried out and, under certain stress conditions, failure is evaluated by fracture pattern analyses. This occurs not only with quasi-static but also with dynamic stress and with different aging states. The knowledge gained will contribute to the reliable and safe bonding of titanium and its alloys. The project is planned in cooperation with the Fraunhofer Institute for Applied Material Research in Bremen.

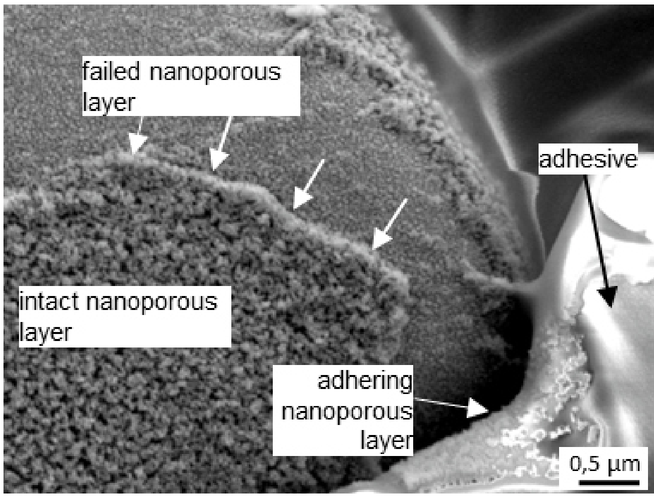

Figure 2: Fracture pattern of a failed adhesive bond on a nanostructured titanium surface.

Dr.-Ing. Martin Kahlmeyer
phone: +49 561 804 - 7567
fax: +49 561 804 - 2045
e-mail: m.kahlmeyer@uni-kassel.de

Prof. Dr.-Ing. Stefan Böhm
phone: +49 561 804 - 3141
fax: +49 561 804 - 2045
e-mail: s.boehm@uni-kassel.de

Research Groups

Implementation, characterization and application of 3-dimensional micro- and nanostructures

3D Self-assembly using Casimir Forces: The applied liquid surface tension brings the two neighboring MEMS shutter blades close to each other, which subsequently get attached to each other by the Casimir force (Fig. 1a). This provides a novel method [1,2] to assemble complex MEMS structures by attaching small parts of overlapping blades through a self-assembly methodology (Fig. 1d-g). If the shutter blade distance is less or equal to 22 nm, the Casimir force would be strong enough for a strong adhesion we found in cooperation with Prof. Buhmann. This means that the attachment force is about 10x stronger than the elastic restoring counterforce since SEM micrographs reveal an average gap distance of about 10 nm. The yield of shutter pairing (Fig. 1c) was studied in detail as a function of the precise sample's orientation during the drying process (Fig. 1b). Currently, intense studies on different metallic sub-layer thicknesses and stress variations lead to adjustable curling radius and identifies for which parameters pairing occurs [3]. Interface roughness influence is also studied intensively.

Functionalized micro- and nanostructures: For many years, structuring and functionalization of 3D micro- and nanostructures have been the main focus of the Technical Electronics department at the Institute for Nanostructure Technology and Analytics. We use the method of nanoimprint lithography (NIL) to create structures with a resolution in the single-digit nanometer range. By implementing guest particles with characteristic properties, functionalized structures or guest-host particle systems can be fabricated (Fig. 2, left) [4-5]. Alternatively, functionalization can also be achieved by using customized imprint resists [6] or by surface modification, for example by coating or sub-structuring the structures which are previously produced via NIL. Both methods of functionalization can be combined and ultimately lead to multifunctionality of the anisotropic particle systems. Such multifunctional particles are required, among others, in sensorics, medical, and materials technology. At the moment they are used as markers or transport vehicles in lab-on-the-chip systems, as drug carriers, or as fillers in composite materials. We focus on further developing the NIL method and testing its limits. E.g., we currently study the imprinting behavior of a hybrid NIL stamp on curved surfaces in cooperation with the Measurement Technology Group of Prof. Lehmann (Fig. 2, center), aiming at a controlled nanostructuring of hemispherical microstructures for the development of novel interference microscopy [7]. In the manufacturing of 3D structures, we especially use the process of two-photon polymerization (2PP). It is a nanoscale additive

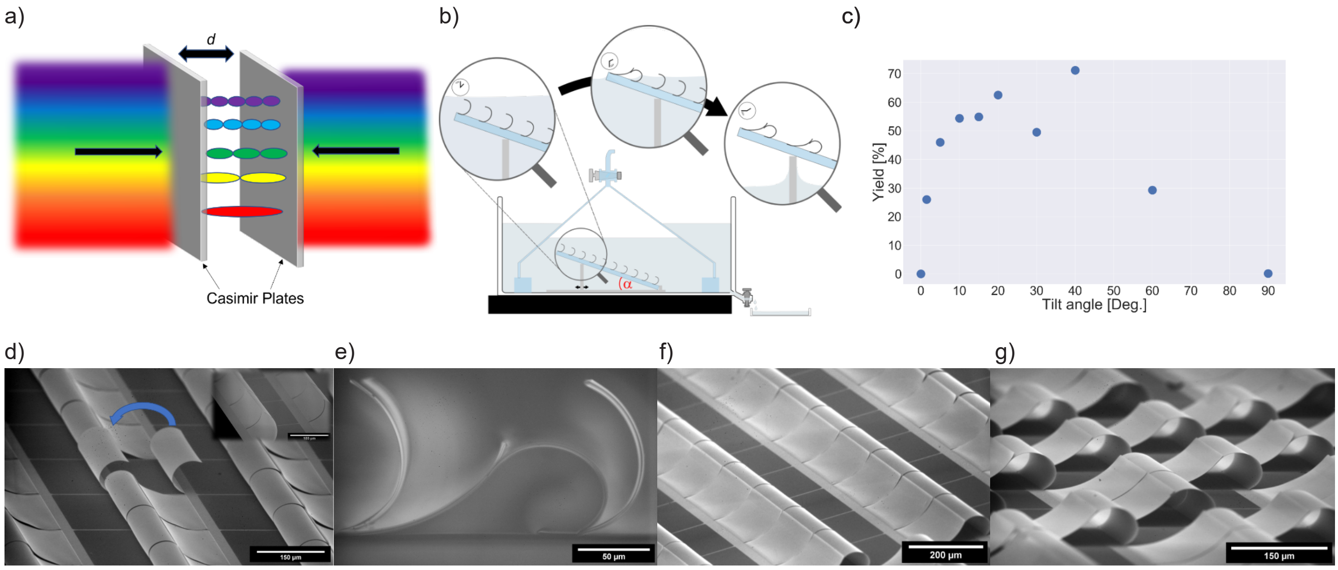

Figure 1: (a) Density of photonic states inside smaller than outside leads to attraction of the 2 shutter blades (plates). (b) Dying process, (c) pairing yield as a function of the tilt angle α. (d,e) Paired and unpaired (f,g) paired shutters.

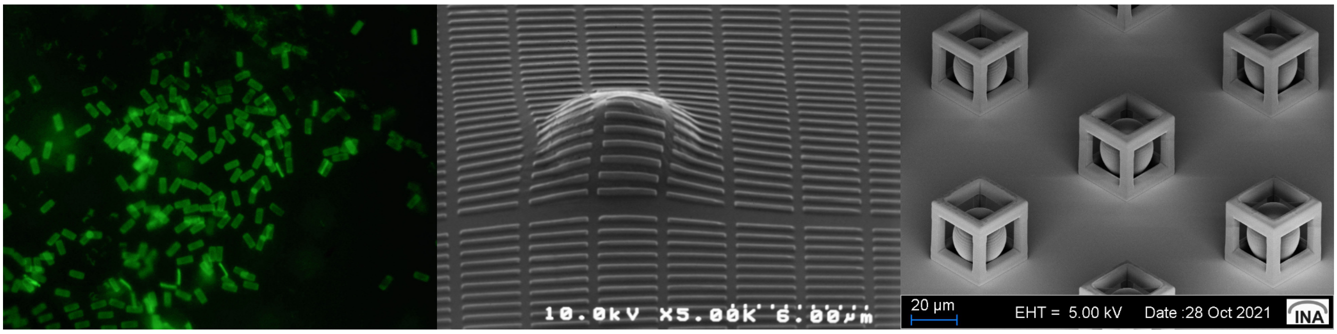

Figure 2: (Left) Fluorescence microscope images of imprinted and released phosphol particles (excitation wavelength: 360-380 nm, emission maximum: 506 nm). (Center) Curved surface, which was sub-structured via NIL. (Right) Geometrically demanding structures can be additively manufactured using two-photon polymerization. Shown here is a ball in a cage, which was fabricated in a single step process.

manufacturing process to produce geometrically demanding polymer structures in a single process step. Analogous to the structures produced by NIL, these structures can also be functionalized. The 2PP method enables the fabrication of highly complex structures that are not accessible using NIL, such as a ball in a cage (Fig. 2, right).

Nanoimprinted Fabry Pérot filter arrays for optical sensing: NIL is also used to fabricate a high-resolution nano-spectrometer combining a Fabry Pérot filter array with a corresponding sensor array. The wavelength of each filter is defined by the individual cavity height sandwiched between two distributed Bragg reflectors (DBRs). 192 individual filter wavelengths on a chip have been implemented [8]. All the individual 3D cavities consist of organic photo-curable NIL resist and are imprinted within a single NIL step. To enable printing over vertical steps between different DBRs, Substrate Conformal Imprint Lithography (SCIL) is applied based on flexible soft stamps ensuring reproduceable imprinting results over large areas. This enables imprinting on different DBRs with different heights and different stopbands. Many flexible soft PDMS stamps can be molded from a single master template (Fig. 3, left). The 3D nanocavities within the soft stamp are filled by capillary forces when in contact with the imprint resist. After curing by UV light, the stamp is removed. Our smallest height difference is 0.2 nm. Since the lateral dimensions of our mesa are still in the range > 6 µm (Fig. 3, right) [8], the chains of the nanoimprint resist molecules spread in lateral directions. Hence, very high vertical resolution can be obtained if larger

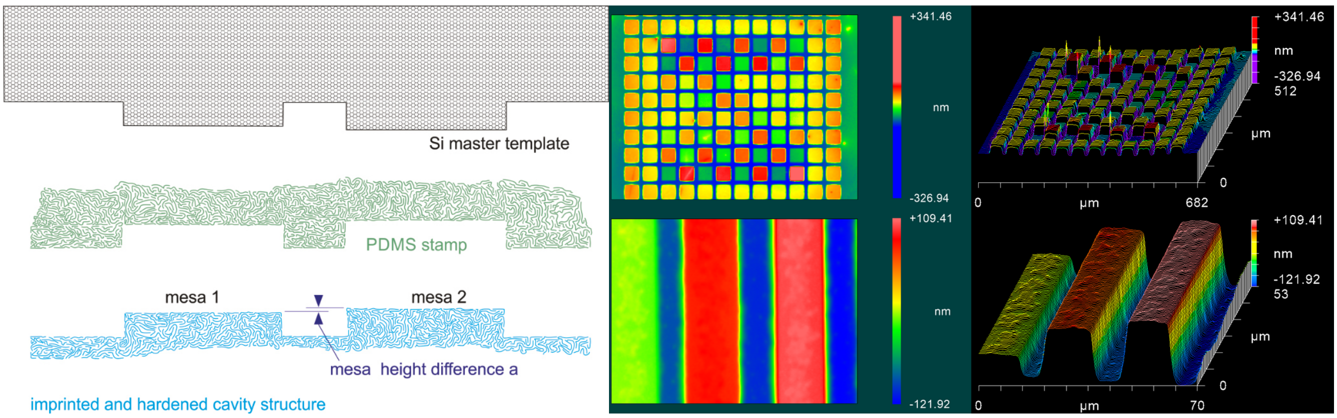

Figure 3 (Left) Fundamentals of molding a stamp from a master template and imprinting two different cavities. (Right) white light interferometry images of the imprinted cavities using SCIL for applications in nanospectrometers in the visible and infrared spectral range.

lateral size can be tolerated - or is even required.

Smart 3D MEMS for light steering and heat management: Today, buildings are responsible for the highest amount of primary energy consumption for heating, cooling, and lighting that triggers rapid global warming, rising sea-level, and profound changes in ocean ecosystems by emitting a massive amount of CO_2. Since 2003, we have studied and developed MEMS smart windows comprising millions of 3D micro- and nanostructured MEMS mirror arrays that can guide and control daylight dynamically [9-12]. The micromirrors are placed inside insulated window glazings filled with an inert gas to guarantee invulnerability to wind, window cleaning, and protection against unfavorable weather conditions. MEMS arrays are fabricated on glass substrates covered by a thin transparent conductive oxide layer (TCO) and an isolation layer. The photoresist layer is structured using photolithography followed by metal layer depositions (all sublayer thicknesses are in the nm range). Additional lithography and deposition steps are performed to locally compensate the induced residual stress on the mirror plane area to obtain flat mirrors. However, the hinge area is left uncompensated to allow deflection of free-standing mirrors vertical to the substrate. A wet chemical lift-off process is executed to remove the sacrificial photoresist, followed by the drying process. The individual micromirrors can be actuated to the horizontal position by applying the full voltage between mirror plane and counter bottom electrode separated by the isolation layer. Several bending angles can be achieved by smaller voltages to balance electrostatic attraction force and elastic counterforce (Fig. 4). We also develop an intelligent networked sensing system to monitor the position of persons, the brightest spot of the sky, temperature distributions, ambient lighting inside the room, and to operate an automated driving circuit enabling various functionalities according to the requirements. With efficient daylight steering and heat management inside the building, MEMS smart windows can save enormous amounts of energy by reducing lighting load throughout the year and heating/ cooling load during summer/winter. Compared to other smart glass, the main features of MEMS smart windows are: the ability to steer light proactively, color neutrality, very long lifetime, safety in case of a power failure, extreme operation temperatures

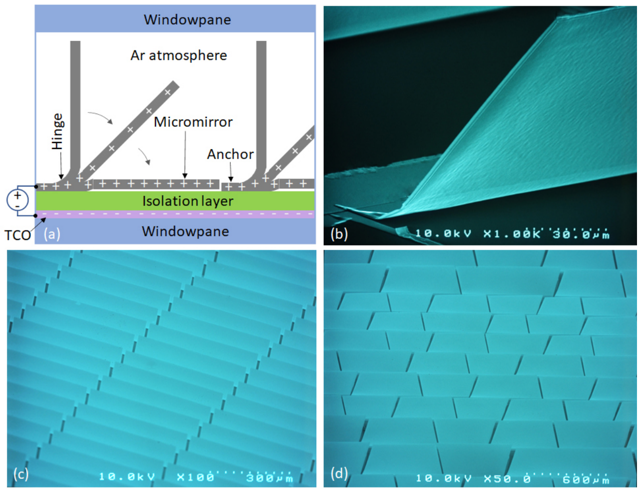

Figure 4: (a) Schematic of electrostatic actuation. Increasing bias voltage, electrostatic attraction force is growing. Different force equilibria between electrostatic attraction force and elastic counterforce provide different actuation angles. Entirely closed states obtained a voltage exceeding the pull-in voltage. SEM micrographs showing (b) planarized free-standing MEMS mirror, regular (c) and irregular mirror arrays (d).

(-80 °C to 120 °C), fast switching (few µs), high contrast T_{max}/T_{min} = 7300, insensitivity against UV radiation and low power consumption down to 0.2 mW/m^2. In addition, low actuation voltages (typically 40 V), clear view through, and independent control of different window areas have also been achieved. Miniaturization into the micro- and nanocosmos is crucial to obtain this performance.

Our working group uses the concept of micro mirror arrays as a platform technology and is currently expanding to polygonal mirror geometries and free forms. When considering alternative shapes, sizes as well as arrangements of MEMS micro mirrors, new possible applications can be aimed. For this purpose, we are developing as well as investigating MEMS ring shutter arrays with subfield addressing enabling the dynamic cutting of sub-fielded, ring-shaped lighting patterns in transmission depicted in Fig. 5. In cooperation with the working group measurement technology of Prof. Lehmann, the integration of those fabricated ring shutter arrays inside Linnik interferometry is planned.

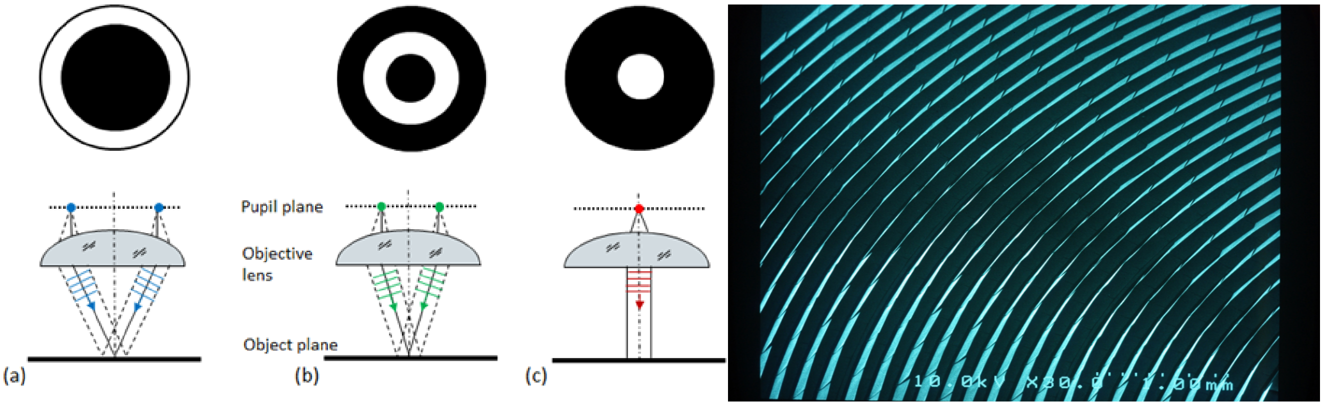

Figure 5: (Left) Application of MEMS ring shutter array inside Linnik interferometry enabling the dynamic cutting of ring-shaped lighting patterns. (Right) SEM image of current MEMS ring shutter array design in top view.

Further information

MEMS = micro-electro-mechanical systems

References

[1] S. Akhundzada, X. Yang, J. Fiedler, E. Käkel, B. Al-Qargholi, S. Buhmann, A. Ehresmann, and H. Hillmer: A novel approach to construct self-assembled 3D MEMS arrays, Microsystem Technologies, 28, 2139-2148 (2022), https://doi.org/10.1007/s00542-022-05361-1 (2022)

[2] P. Kästner, E. Käkel, S. Akhundzada, R. Donatiello and H. Hillmer, Development of self-assembled 3D MEMS Paired Shutter Arrays for studies on Casimir forces, Technical Digest MOC 2022, #1054, p. 74-75 (2022).

[3] Elsaka, B.; Kästner, P.; Käkel, E.; Donatiello, R.; Hillmer, H. Investigation of the Influence of Sublayer Thickness on Pairing of Metallic MEMS Shutter Blades. Appl. Sci. 2023, 13, 1538. https://doi.org/10.3390/app13031538

[4] U-M. Ha, B. Kaban, A. Tomita, K. Krekić, D. Klintuch, R. Pietschnig, A. Ehresmann, D. Holzinger, H. Hillmer: Multifunctional guest–host particles engineered by reversal nanoimprint lithography. In: Applied Nanoscience, Vol. 8: Issue 5, pp. 1161–1169 (2018)

[5] F. Roesler, B. Kaban, D. Klintuch, U. Ha, C. Bruhn, H. Hillmer, R. Pietschnig: Tailoring Phospholes for Imprint of Fluorescent 3D Structures. In: European Journal of Inorganic Chemistry, (2019). DOI: https://doi.org/10.1002/ejic.201900742

[6] D. Löber, S. Dey, B. Kaban, F. Roesler, M. Maurer, H. Hillmer, R. Pietschnig: 3D Micro/Nanopatterning of a Vinylferrocene Copolymer. In: Molecules, 25(10), 2438, (2020). DOI: https://doi.org/10.3390/molecules25102438

[7] B. Allendorf, E. Käkel, U. Ha, S. Hagemeier, H. Hillmer, P. Lehmann: Adaptive high-resolution Linnik interferometry for 3D measurement of microparticles. In: Optics Letters Vol. 44, Issue 14, pp. 3550-3553, (2019). DOI: https://doi.org/10.1364/OL.44.003550

[8] H. Hillmer, C. Woidt, A. Kobylinskiy, M. Kraus, A. Istock, M.S. Q. Iskhandar, R. Brunner and T. Kusserow: Miniaturized interferometric sensors with spectral tunability for optical fiber technology – a comparison of size requirements, performance, and new concepts. PHOTONICS 8, 332 (2021). DOI:10.3390/photonics8080332

[9] H. Hillmer, J. Schmid, I. Stadler, Micro Mirror Arrays, Patents EU 1700152B1, US 7677742B2, DE 10358967B4

[10] M. S. Iskhandar, B. Al-Qargholi, M. M. Khan, A. Tatzel, H. Luo, S.Nazemroaya, Q. Li, and H. Hillmer, Development of optical MEMS-based micromirror arrays for smart window applications:Implementation of subfield addressing and reliability measurements, Yearbook surface technology, Leuze publishing house, Vol. 52, pp. 93-107, 2019, ISBN number 978-3-87480-357-1.

[11] S. Nazemroaya, M. Iskhandar, Md K. Hasan, Q. Li, H. Hillmer: Concepts for clear view through 3D structured surfaces of MEMS smart glass: design, implementation, characterization and validation, Yearbook surface technology, Leuze publishing house, Vol. 76, pp. 101-115, 2020, ISBN: 978-3-87480-364-9

[12] H. Hillmer, M.S.Q. Iskhandar, M. K. Hasan, S. Akhundzada, B. Al-Qargholi, & A. Tatzel, MOEMS micromirror arrays in smart windows for daylight steering, invited opening article, Journal of Optical Microsystems, 1(1), 014502, 2021

Group photo of the technological electronics group

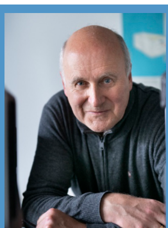

Prof. Dr. Hartmut Hillmer
phone: +49 561 804 - 4485
e-mail: hillmer@ina.uni-kassel.de

Awards

Cooperation with the University of Chemical Technology and Metallurgy, Sofia, Bulgaria

The educational and scientific collaboration between the University of Kassel and the University of Chemical Technology and Metallurgy (UCTM), Sofia, Bulgaria, continues already 25 years. In this period 24 students from different departments of UCTM related to Materials Science and Engineering have visited Kassel for one semester. The exchange students prepare their master theses employing the facilities of several CINSaT groups supervised by scientists from the host groups. The visits are financially supported by the Erasmus program of EC or by the German Academic Exchange Service (DAAD). DAAD sponsors a study program in chemical engineering at UCTM, taught completely in German. From German side the coordination of the program is provided by the Technical University of Hamburg-Harburg, other partners in it are the University of Kassel, Otto-von-Guericke-University of Magdeburg, and Leibniz University of Hannover, which not only host students from UCTM, but also provide lectures, seminars, and lab courses at UCTM in Sofia.

In occasion of the 70th anniversary of UCTM, the Academic Council acknowledged the educational support from the German partner universities. At a solemn session on May 22, 2023, the Rector of UCTM, Prof. Dr. Senya Terzieva-Zhelyazkova awarded representatives of these universities, among them Prof. Cyril Popov, and as well as her excellency the ambassador of Germany in Bulgaria Irene Maria Plank for their long-year contribution to the development of bilateral scientific and educational connections. In his gracious speech, Prof. Popov thanked the Academic Council of UCTM for the award and assured the continuation of the collaboration in the next years, including also update of the curriculum based on the experience of CINSaT in interdisciplinary study programs.

Prof. Senya Terzieva-Zhelyazkova, Rector of UCTM and Prof. Cyril Popov at the awarding ceremony

After the awarding ceremony: Prof. Cyril Popov with Prof. Senya Terzieva-Zhelyazkova, Rector of UCTM, and her excellency Irene Maria Plank, ambassador of Germany in Bulgaria, and her secretary (from right to left)

Latest Reports

CINSaT Spring Colloquium 2023

The 2023 spring colloquium in Friedrichroda is the first to break the 100-participant mark.

Once again, the activities of the CINSaT in 2023 started with the annual CINSaT spring colloquium in the AHORN Berghotel in Friedrichroda. With increasing member numbers, it was foreseeable that the number of participants would rise too and with a little over 100 participants we could welcome more participants than ever before. The program was packed with over 20 scientific talks given in dedicated focal point sessions and we can additionally report a new record with over 60 poster contributions closing into the capacity limits of the venue. We want to thank once again all speakers and poster creators who contributed heavily to the success of the event.

The speaker of the CINSaT, Prof. Reithmaier, opened the colloquium and welcomed all participants on the first day and handed over to Prof. Hillmer who chaired the first session about 3-dimensional nanostructures handing over to Prof. Müller, chairing the multiscale bioimaging session. After lunch the audience was listening to a 1-hour talk by Prof. Adrian Mellage entitled "Capturing and quantifying reactive transport in groundwater: The 'invisible' rock-water interface" given in the scope of his application as an associated CINSaT member. Prof. Demekhin chaired the last session of the day about chiral systems. Following a short break and taking the obligatory group photo, some of the participants seized the opportunity to take a hike in the forests around the hotel before dinner. In the evening everyone gathered for the poster session which gave enough room for individual discussions about recent results and possible collaborations in the future.

The second day started with a continuation of the scientific talks, starting with the photonics session chaired by Prof. Lehmann followed by Prof. Middendorf who chaired the nanomaterials session. Before lunch, Prof. Guido Falk von Rudorff gave his application talk entitled "Computational material design and the curse of dimensionality". He also applied for the associated CINSaT membership. The last lecture session of the colloquium was chaired by Prof. Singer about quantum technology. In the following the participants were divided according to their research in six focus sessions giving the opportunity to discuss issues or problems in more detail with peers that work in the same area. The colloquium was closed by Prof. Reithmaier in the afternoon and we as organizers hope that all participants left with solutions to their problems, new insights, and ambitious ideas!

Audience of this years CINSaT spring colloquium.

Focus session of the 3-dimensional nanostructures focal point chaired by Prof. Dr. Hillmer

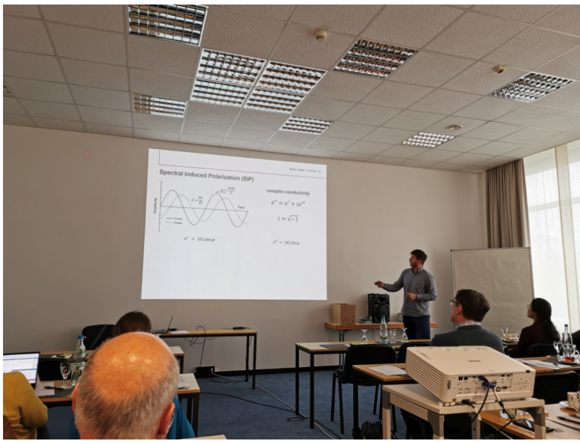

Presentation by associated CINSaT member applicant Prof. Dr. Adrian Mellage

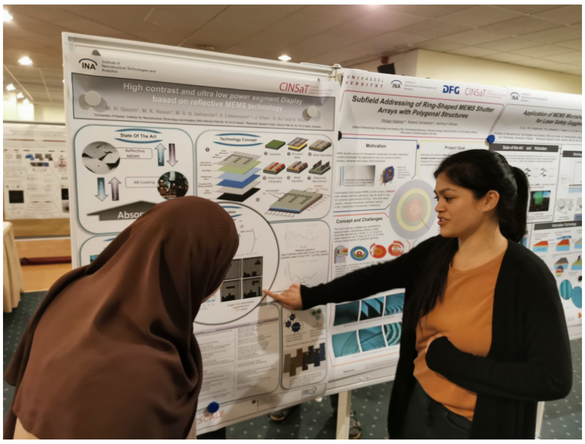

Poster session in the evening of the first day.

Focus session of the nanomaterials focal point chaired by Prof. Dr. Middendorf

Presentation by associated CINSaT member applicant Prof. Dr. Guido Falk von Rudorff

Group photo of the participants.

Nano Arts

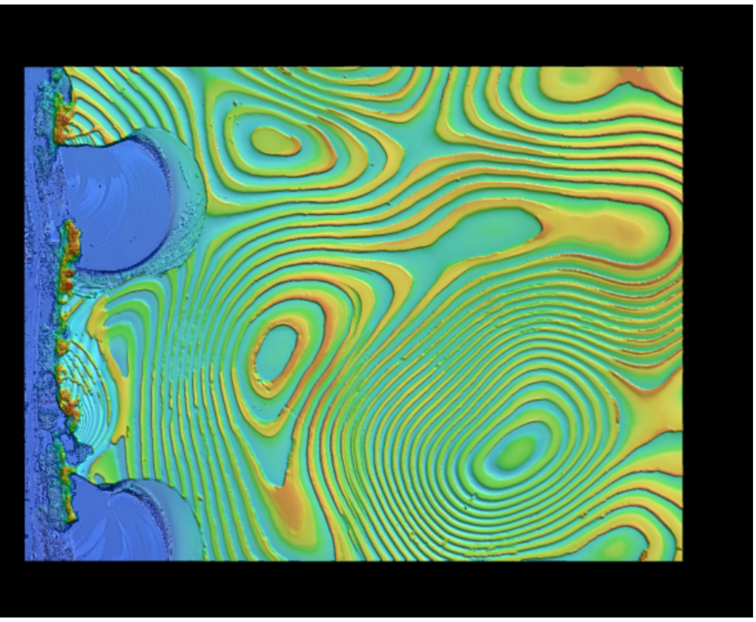

Images taken with CLSM of a rough surface of photoresist using confocal laser mode.

Image taken by Basma Elsaka

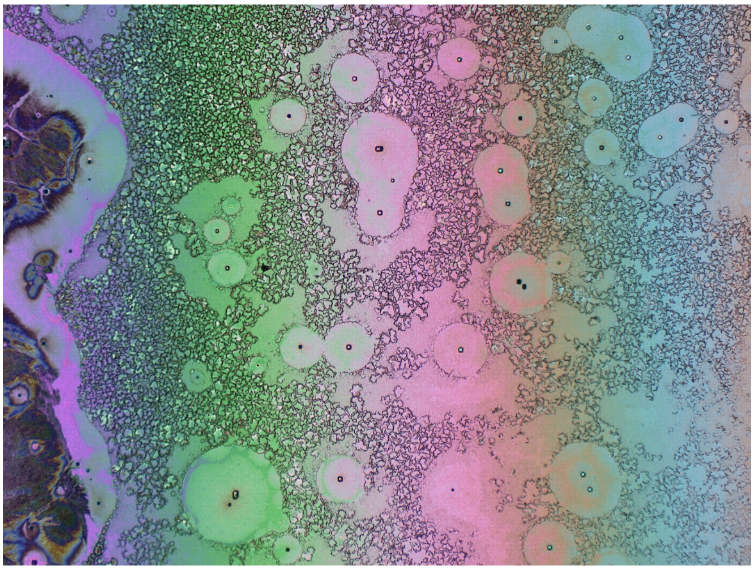

Edges of a UNCD coated 3 inch Si wafer. The colors stemming from interferences caused by variation of the UNCD layer thickness which is especially pronounced on the edges of the wafer.

Image taken by Daniel Merker

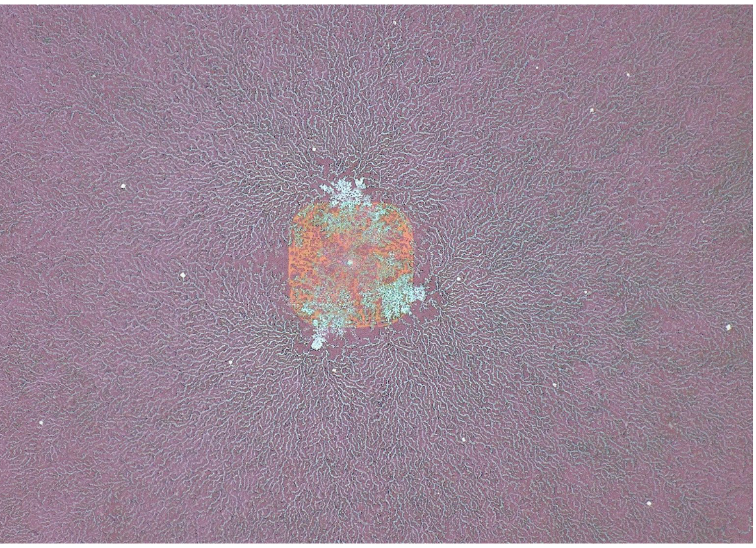

Magnification on one of the dots in the image above. The sample was treated with various deposition and etching steps (wet and dry) leading to the occurence of this peculiar shapes. 3D scans reveal that the squared dots are actually holes of roughly 1.5 µm depth with a pyramidical shape.

Image taken by Daniel Merker

The SEM image is showing a section of a ring-shaped micro shutter array. High stress-induced bending of each micro shutter blade leads to partial break of the anchors. The resulting shape is giving the impression of bat or angel wings – that's in the eye of the beholder.

Image taken by Philipp Kästner

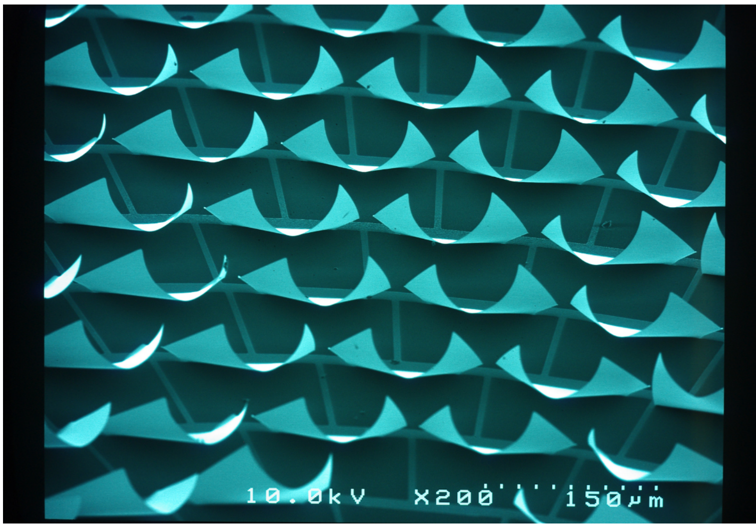

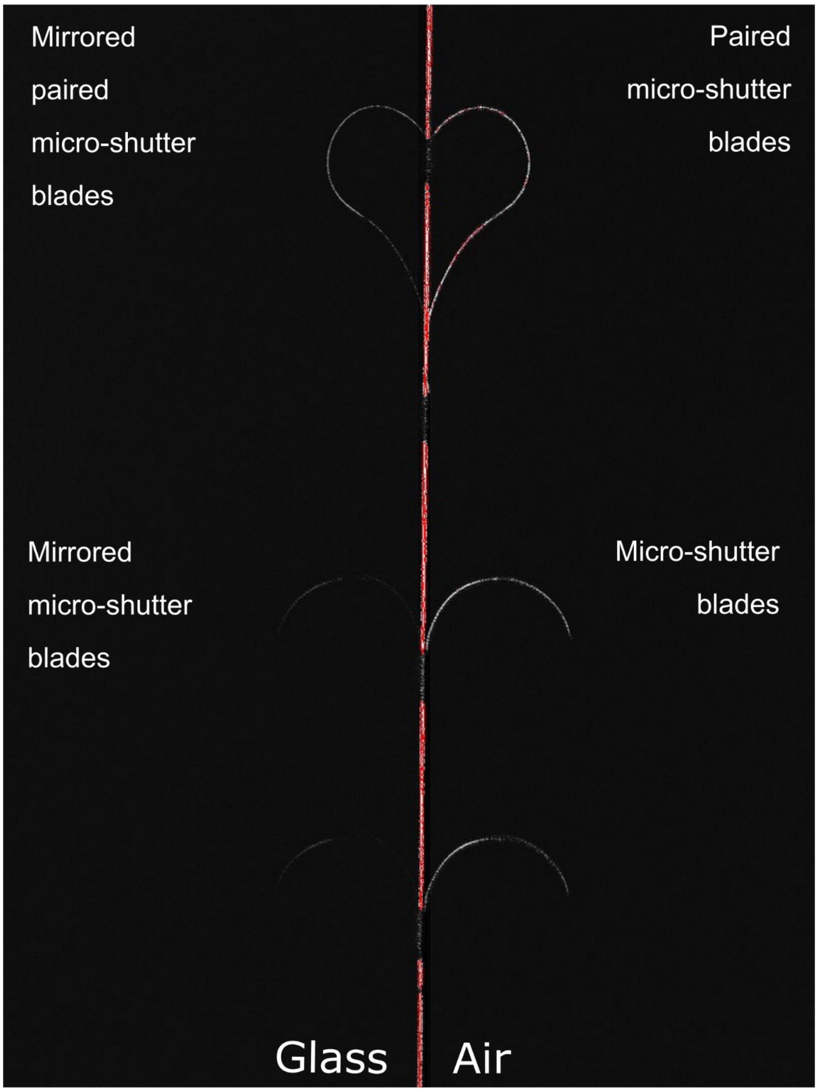

Heart on a string paired micro-shutter blades are forming a heart when they are mirrored across the substrate plane (CLSM Image).

Image taken by Eireen Käkel

Photo: Campus Heinrich-Plett-Straße, Press and Public Relations Office University of Kassel, Studio Blåfield

Imprint

address
University of Kassel
Center for Interdisciplinary Nanostructure Science and Technology (CINSaT)
Heinrich-Plett-Straße 40
34132 Kassel

contact:
phone: +49 561 804-4384
e-mail: info@cinsat.uni-kassel.de
website: www.cinsat.de

editorial:
Prof. Dr. Johann Peter Reithmaier
Dr. Daniel Merker

layout:
Dr. Daniel Merker
Florian Ott

print:
viaprinto
Martin-Luther-King-Weg 30a
48155 Münster

Responsible according to press law (german: ViSdPR):
CINSaT executive board,
University of Kassel